Spatial chirp revisited: Matrix analysis of dispersionless optical systems and correct interferometric autocorrelation

Nikolay Dimitrov, Nedyalko Chakarov, Alexander Dreischuh*
Department of Quantum Electronics, Faculty of Physics, Sofia University,
5, J. Bourchier Blvd., BG-1164 Sofia, Bulgaria

ABSTRACT

In this work, by using 4x4 ray-pulse matrices, we analyze the influence of the position of the output diffraction grating in 4*f*- and 2*f*-2*f*-systems with respect to the eventually introduced group-delay dispersion, spatial and angular chirp. We show that in the 4*f*-configuration, in contrast to the 2*f*-2*f*-setup, the grating offset does not cause angular chirp and pulse front tilt. We theoretically derive an expression for the interferometric autocorrelation signal in the presence of an arbitrary pulse-front tilt.
Keywords: Matrix methods in paraxial optics, pulse front tilt, ultrafast measurements

1. INTRODUCTION

Dispersionless 4*f*- and 2*f*-2*f*-setups[1,2] are frequently used for various pulse shaping applications including creation of spatial phase singularities in broadband femtosecond beams/pulses[3,4]. Eventual misalignments in such systems are expected to result in spatial and angular chirp, uncompensated group-delay dispersion and time-vs.-angle coupling. In this work we first analyze the influence of the position of the output diffraction grating in both 4*f*- and 2*f*-2*f*-systems. The calculations are based on the 4x4 ray-pulse matrices introduced by Kostenbauder[5] and generalized by Duarte[6] and Trebino and co-workers[7]. In essence, the 4x4 matrices connect the input and output ray and pulse coordinates to each other. The spatial and temporal characteristics of the pulse are represented in a ray-pulse vector $(x, \theta, t, f)^T$. The spatial coordinates position (x) and slope (θ) are the same as in the ordinary 2x2 matrices. The coordinate system is defined by the path of a diffraction limited reference beam of a central hertzian frequency f and, when thought of as being temporally transform-limited, can mark a well-defined arrival time at each transverse plane[5]. In terms of such coordinates and using a 4x4 matrix, the action of an optical element can be described as

$$\begin{pmatrix} x_{out} \\ \vartheta_{out} \\ t_{out} \\ f_{out} \end{pmatrix} = \begin{pmatrix} A & B & 0 & \dfrac{\partial x_{out}}{\partial f_{in}} \\ C & D & 0 & \dfrac{\partial \vartheta_{out}}{\partial f_{in}} \\ \dfrac{\partial t_{out}}{\partial x_{in}} & \dfrac{\partial t_{out}}{\partial \vartheta_{in}} & 1 & \dfrac{\partial t_{out}}{\partial f_{in}} \\ 0 & 0 & 0 & 1 \end{pmatrix} \begin{pmatrix} x \\ \vartheta \\ t \\ f \end{pmatrix}_{in} = \begin{pmatrix} A & B & 0 & E \\ C & D & 0 & F \\ G & H & 1 & I \\ 0 & 0 & 0 & 1 \end{pmatrix} \begin{pmatrix} x \\ \vartheta \\ t \\ f \end{pmatrix}_{in} \tag{1}$$

where A, B, C, and D are the components of the 2x2 ray matrix, $E=\partial x_{out}/\partial f_{in}$ and $F=\partial \vartheta_{out}/\partial f_{in}$ describe the spatial and angular chirp, respectively, whereas $H=\partial t_{out}/\partial \vartheta_{in}$ and $I=\partial t_{out}/\partial f_{in}$ stand for the time-vs.-angle coupling and the group delay dispersion, and $G=\partial t_{out}/\partial x_{in}$ is related to the pulse front tilt angle α via [8]

$$\tan(\alpha) = \frac{\partial (c t_{out})}{\partial x_{out}} = c \frac{\partial t_{out}}{\partial x_{in}} \frac{\partial x_{in}}{\partial x_{out}} = cG \frac{\partial x_{in}}{\partial x_{out}} \tag{2}$$

where c is the speed of light.

*ald@phys.uni-sofia.bg; phone (+359-2) 8161-611; fax (+359-2) 868-8813; www.phys.uni-sofia.bg

15th International School on Quantum Electronics: Laser Physics and Applications, edited by Tanja Dreischuh
Elena Taskova, Ekaterina Borisova, Alexander Serafetinides, Proceedings of SPIE Vol. 7027, 70271K
 · doi: 10.1117/12.822533

2. MATRIX ANALYSIS OF DISPERSIONLESS OPTICAL SYSTEMS

2.1 Analysis of a 4*f*-system

In Fig. 1 we show a sketch of the analyzed 4*f*-system. We assume that the two identical gratings are precisely aligned with their grooves being parallel. The only deviation from the precise 4*f* alignment we consider is a shift Δ of one of the gratings away from the focus of the respective lens.

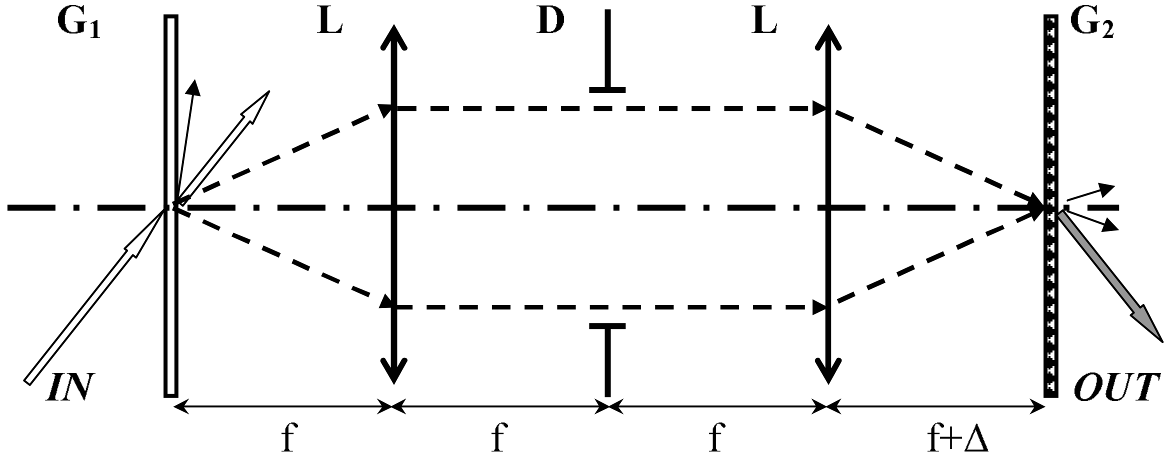

Fig. 1. Sketch of the analyzed 4*f*-system. G_1, G_2 – diffraction gratings assumed to be aligned with strictly parallel grooves, L – lenses of a focal length f, D – diaphragm, Δ – grating offset from the perfect 4*f* alignment.

In the rest of this paper f and f_0 stand for the lens focal length and the central hertzian frequency of the pulse spectrum, respectively. According to the procedure of the matrix analysis one has to multiply the respective ray-pulse matrices in reverse order (from the exit to the entrance), i.e.

$$M_{4f} = G_2.T_{f+\Delta}.F.T_{2f}.F.T_f.G_1 \tag{3}$$

The explicit form of the matrices for the diffraction gratings (note the change in the incident-ray-to-grating-surface and reflected-ray-to-grating-surface angles ψ and ϕ) are

$$G_1 = \begin{pmatrix} -\dfrac{\sin(\phi)}{\sin(\psi)} & 0 & 0 & 0 \\ 0 & -\dfrac{\sin(\psi)}{\sin(\phi)} & 0 & \dfrac{\cos(\phi)-\cos(\psi)}{f_0\sin(\phi)} \\ \dfrac{\cos(\psi)-\cos(\phi)}{c\sin(\psi)} & 0 & 1 & 0 \\ 0 & 0 & 0 & 1 \end{pmatrix}, \quad G_2 = \begin{pmatrix} -\dfrac{\sin(\psi)}{\sin(\phi)} & 0 & 0 & 0 \\ 0 & -\dfrac{\sin(\phi)}{\sin(\psi)} & 0 & \dfrac{\cos(\psi)-\cos(\phi)}{f_0\sin(\psi)} \\ \dfrac{\cos(\phi)-\cos(\psi)}{c\sin(\phi)} & 0 & 1 & 0 \\ 0 & 0 & 0 & 1 \end{pmatrix}.$$

The transition matrices have the much simpler form

$$T_f = \begin{pmatrix} 1 & f & 0 & 0 \\ 0 & 1 & 0 & 0 \\ 0 & 0 & 1 & 0 \\ 0 & 0 & 0 & 1 \end{pmatrix}, \quad T_{2f} = \begin{pmatrix} 1 & 2f & 0 & 0 \\ 0 & 1 & 0 & 0 \\ 0 & 0 & 1 & 0 \\ 0 & 0 & 0 & 1 \end{pmatrix}, \quad T_{f+\Delta} = \begin{pmatrix} 1 & f+\Delta & 0 & 0 \\ 0 & 1 & 0 & 0 \\ 0 & 0 & 1 & 0 \\ 0 & 0 & 0 & 1 \end{pmatrix}, \text{ and } F = \begin{pmatrix} 1 & 0 & 0 & 0 \\ -1/f & 1 & 0 & 0 \\ 0 & 0 & 1 & 0 \\ 0 & 0 & 0 & 1 \end{pmatrix}.$$

In this way we arrive at the matrix M_{4f} of the modeled 4*f*-system

$$M_{4f} = \begin{pmatrix} -1 & -\Delta\dfrac{\sin^2(\psi)}{\sin^2(\phi)} & 0 & \Delta\dfrac{\left(\cos(\phi)-\cos(\psi)\right)\sin(\psi)}{f_0\sin^2(\phi)} \\ 0 & -1 & 0 & 0 \\ 0 & \Delta\dfrac{\left(\cos(\phi)-\cos(\psi)\right)\sin(\psi)}{c\sin^2(\phi)} & 1 & -\Delta\dfrac{\left(\mathrm{cotg}(\phi)-\cos(\psi)/\sin(\phi)\right)^2}{cf_0} \\ 0 & 0 & 0 & 1 \end{pmatrix}. \tag{4}$$

It is evident that the misalignment Δ of the grating determines the signs of the introduced group-delay dispersion (GDD), spatial chirp (SC) and time-vs.-angle coupling (TvAC):

$$GDD = \frac{\partial t_{out}}{\partial f_{in}} = -\frac{\Delta}{cf_0}\left[\mathrm{cotg}(\phi)-\cos(\psi)/\sin(\phi)\right]^2 \ , \tag{5a}$$

$$SC = \frac{\partial x_{out}}{\partial f_{in}} = \frac{\Delta\left[\cos(\phi)-\cos(\psi)\right]\sin(\psi)}{f_0\sin^2(\phi)} \ , \tag{5b}$$

$$TvAC = \frac{\partial t_{out}}{\partial \vartheta_{in}} = \Delta\frac{\left[\cos(\phi)-\cos(\psi)\right]\sin(\psi)}{c\sin^2(\phi)} \ . \tag{5c}$$

Since in M_{4f} (see Eq. 4) the matrix elements F=0 and G=0, this misalignment does not introduce angular chirp and pulse front tilt.

2.2 Analysis of a 4*f*-system

Sketch of the analyzed $2f$-$2f$ system is shown in Fig. 2. The notations are the same as in Fig. 1, except the additional notations of the different diffracted-order beams.

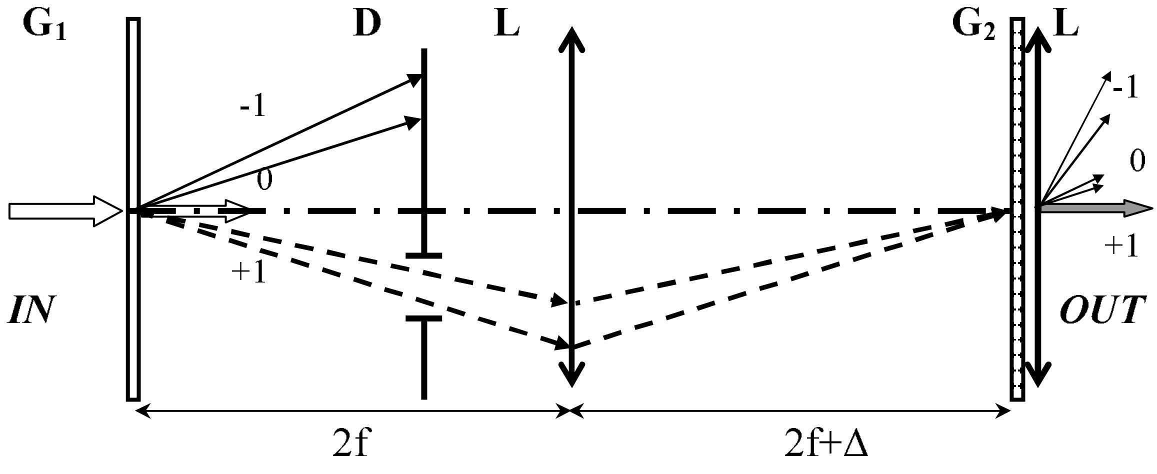

Fig. 2. Sketch of the analyzed $2f$-$2f$-system. G_1, G_2 – diffraction gratings assumed to be aligned with strictly parallel grooves, L – lenses of a focal length f, D – diaphragm, Δ – grating-lens-pair offset from the exact $2f$ distance.

Multiplying the matrices of the individual optical elements in the following (reverse) order

$$M_{2f\text{-}2f} = F.G_2.T_{2f+\Delta}.F.T_{2f}.G_1 \tag{6}$$

with matrices G_1, G_2, F and T_{2f} being the same as in the previous case, and

$$T_{2f+\Delta}=\begin{pmatrix}1 & 2f+\Delta & 0 & 0\\ 0 & 1 & 0 & 0\\ 0 & 0 & 1 & 0\\ 0 & 0 & 0 & 1\end{pmatrix}$$

we derive the matrix $M_{2f\text{-}2f}$ of the misaligned $2f$-$2f$ system

$$M_{2f-2f}=$$

$$\begin{pmatrix}-\frac{\Delta+f}{f} & -\Delta\frac{\sin^2(\psi)}{\sin^2(\phi)} & 0 & \Delta\frac{\left(\cos(\phi)-\cos(\psi)\right)\sin(\psi)}{f_0\sin^2(\phi)}\\ \frac{\Delta+f-f\sin^2(\phi)/\sin^2(\psi)}{f^2} & -1+\Delta\frac{\sin^2(\psi)}{f\sin^2(\phi)} & 0 & -\Delta\frac{\left(\text{cotg}(\phi)-\cos(\psi)/\sin(\phi)\right)\sin(\psi)}{ff_0\sin(\phi)}\\ -\Delta\frac{\left(\text{cotg}(\psi)-\cos(\phi)/\sin(\psi)\right)}{cf} & \Delta\frac{\left(\cos(\phi)-\cos(\psi)\right)\sin(\psi)}{c\sin^2(\phi)} & 1 & -\Delta\frac{\left(\text{cotg}(\phi)-\cos(\psi)/\sin(\phi)\right)^2}{cf_0}\\ 0 & 0 & 0 & 1\end{pmatrix}. \quad (7)$$

As seen, in this case the grating-lens-pair misalignment has much more complicated consequences. Comparing Eqs. 4 and 7 one can see that equal misalignments of the systems result in equal group-delay dispersion (GDD, Eq. 5a), spatial chirp (SC, Eq. 5b) and time-vs.-angle coupling (TvAC, Eq. 5c). The misalignment introduces however a pulse-front-tilt (PFT)

$$PFT=\frac{\partial t_{out}}{\partial x_{in}}=-\Delta\frac{\text{cotg}(\psi)-\cos(\phi)/\sin(\psi)}{cf}\ . \quad (8)$$

This later pulse distortion, which is especially important for nearly single-cycle ultrashort optical pulses, is understood[8] as an arrival time difference t_{out} which depends on the transverse beam coordinate x_{out}. In a misaligned $2f$-$2f$-system the corresponding pulse front tilt angle α is given by

$$\tan(\alpha)=\frac{\partial(ct_{out})}{\partial x_{out}}=c\frac{\partial t_{out}}{\partial x_{in}}\frac{\partial x_{in}}{\partial x_{out}}=\frac{\Delta}{f+\Delta}\left[\text{cotg}(\psi)-\cos(\phi)/\sin(\psi)\right]\ . \quad (9)$$

3. AUTOCORRELATION SIGNAL IN THE PRESENCE OF PULSE FRONT TILT

In this section we consider Gaussian beam/pulse of width x_0 and duration t_0. When there is no pulse front tilt, the electric field of this wave is described by

$$E(x,t)=E_0\exp\left[-\left(x/x_0\right)^2-\left(t/t_0\right)^2\right]\exp\left(i\omega t\right)\ . \quad (10)$$

Fig. 3 is intended to visualize the difference between pulses without and with pulse front tilt. The right frame in Fig. 3 correctly corresponds to the understanding that, at a fixed plane perpendicular to the beam propagation direction, an arrival time difference depending on the transverse beam coordinate means presence of a spatial chirp. In a standard Michelson-type autocorrelator the pulse front tilt remains hidden [9] (see Fig. 4, left). The picture drastically changes when one of the beams is rotated in space at 180° (Fig. 4, right). Setups for an interferometric inverted field autocorrelation suited for the detection of tilted pulse fronts are known[9,10]. Our goal in this section is to derive an analytic expression for the interferometric autocorrelation signal for arbitrary large pulse front tilt.

Starting with the optical field amplitudes E_1 and E_2 of the beams/pulses with opposite pulse front tilts $-\alpha$ and α, respectively, the intensity $I_{2\omega}$ of the second harmonic that is generated during the autocorrelation is

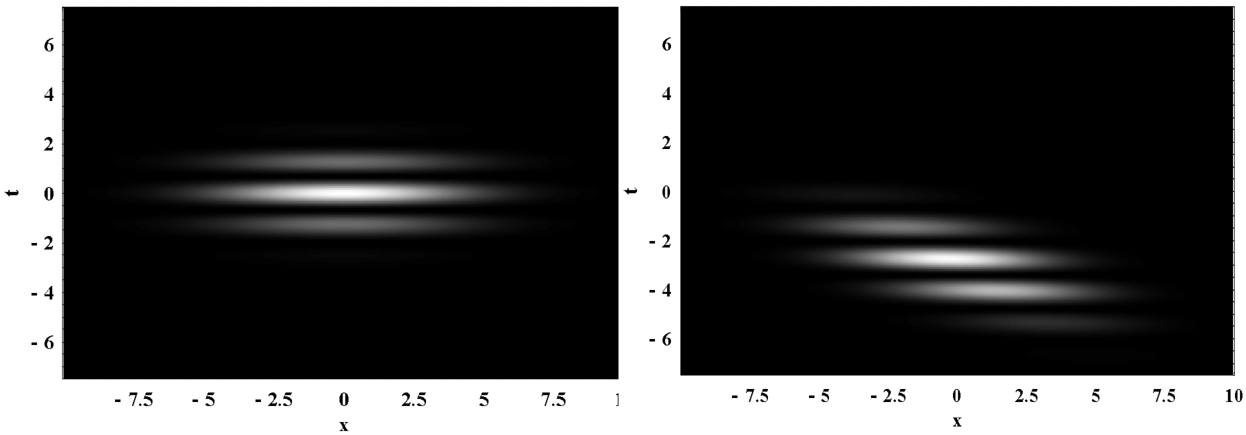

Fig. 3. Electric field amplitude of an ultrashort pulse without (left) and with pulse front tilt (right).

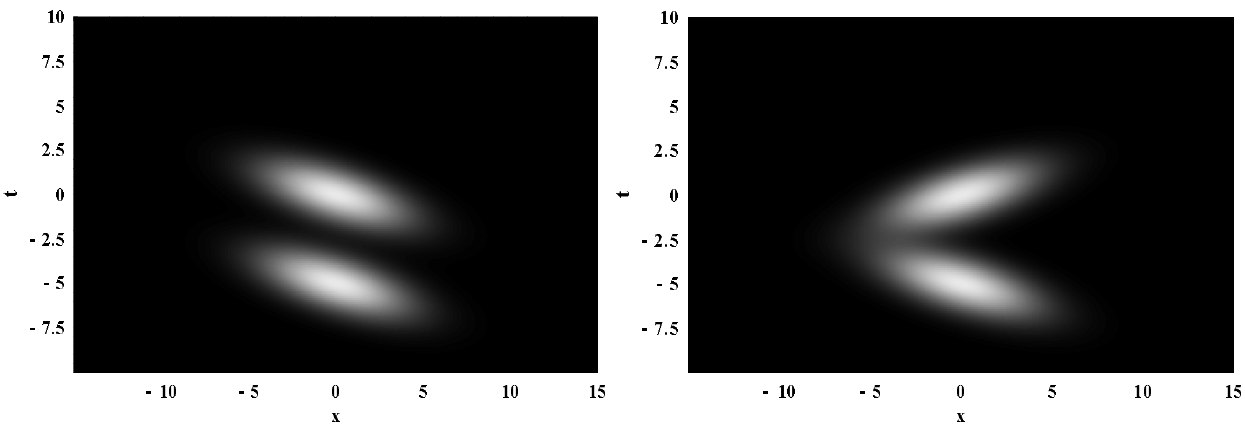

Fig. 4. Electric field amplitude of an ultrashort pulse with pulse front tilt propagating in a standard Michelson-type autocorrelator (left) and in an autocorrelator, in which one of the beams is rotated in space at 180° (right).

$$I_{2\omega}\left(x,t,\alpha,\tau_d\right)=\left|E_{2\omega}\left(x,t,\alpha,\tau_d\right)\right|^2=\left|\left(E_1(x,t,-\alpha)+E_2(x,t,\alpha,\tau_d)\right)^2\right|^2 . \tag{11}$$

τ_d is the time delay between the pulses during the autocorrelation. With a wide aperture photodetector and a detector rise time much longer than the typical pulse length (conditions easily fulfilled with ultrashort pulses) the normalized correlation signal has the form

$$P_{2\omega}^{AK}\left(\alpha,\tau_d\right)=\frac{\int_{-\infty}^{\infty}\int_{-\infty}^{\infty}I_{2\omega}\left(x,t,\alpha,\tau_d\right)dxdt}{2\int_{-\infty}^{\infty}\int_{-\infty}^{\infty}\left|\left(E_i(x,t,\alpha,\tau_d)\right)^2\right|^2 dxdt} , \tag{12}$$

where i=1,2. The natural normalization to the energy of the second harmonic signal generated from each pulse separately yields a correlation peak-to-background ratio of 8:1 at zero tilt of the pulse front. The most time-consuming but straightforward step in this analysis is the correct rotation of the electric field amplitude (10) at an angle -α and α, respectively. Following the procedure described above, we derived general expression for the interferometric autocorrelation signal for arbitrary large pulse front tilt α

$$P_{2\omega}^{AK}(\alpha,\tau_d)=1+2\sqrt{2}x_0t_0\left(\frac{8\exp\left\{-\frac{A(\alpha)}{B(\alpha)}\tau_d^2\right\}cos[\omega\tau_d]}{\sqrt{B(\alpha)}}+\frac{\exp\left\{-\frac{1}{C(\alpha)}\tau_d^2\right\}(2+cos[2\omega\tau_d])}{\sqrt{D(\alpha)}}\right), \tag{13}$$

where

$$\begin{aligned}
A(\alpha)&=12\left[(x_0^2+t_0^2)+(x_0^2-t_0^2)cos(2\alpha)\right]\\
B(\alpha)&=3x_0^4+26x_0^2t_0^2+3t_0^4-3(x_0^2-t_0^2)^2cos(4\alpha)\\
C(\alpha)&=t_0^2cos^2(\alpha)+x_0^2sin^2(\alpha)\\
D(\alpha)&=x_0^4+6x_0^2t_0^2+t_0^4-(x_0^2-t_0^2)^2cos(4\alpha)
\end{aligned} \tag{14}$$

In Fig. 5 we show numerically calculated interferometric autocorrelation signals $P_{2\omega}^{AK}$ for different values of α. It is evident that the correlation peak-to-background signal ratio of 8:1 for α=0 gradually decreases with increasing α, whereas the amplitudes of the side lying peaks grow monotonically. This is a clear indication that the autocorrelation curve broadens with increasing the pulse front tilt. The effect is better pronounced when we inspect the envelopes of the autocorrelation signals (see Fig. 6). It is intuitively clear that, at one and the same beam width, the shorter the laser pulse, the stronger the influence of the pulse front tilt. Table 1 summarizes results concerning the relative pulse broadening $\Delta t/\Delta t(\alpha=0)$ for different pulse duration to beam width ratios vs. tilt angle α. As seen, for α=0.35rad a decrease of the pulse duration by a factor of 3 results in an increase of the effective pulse broadening by a factor of more than 2. The shorter pulses appear stronger influenced by the pulse front tilt α than the longer ones.

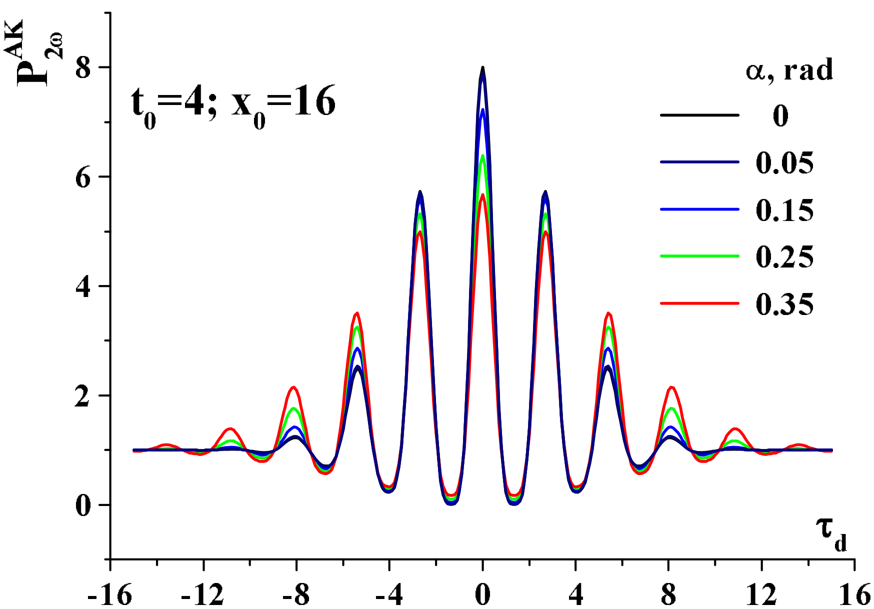

Fig. 5. Simulated interferometric atocorrelation signal (Eq. 13) for different values of the pulse front tilt α.

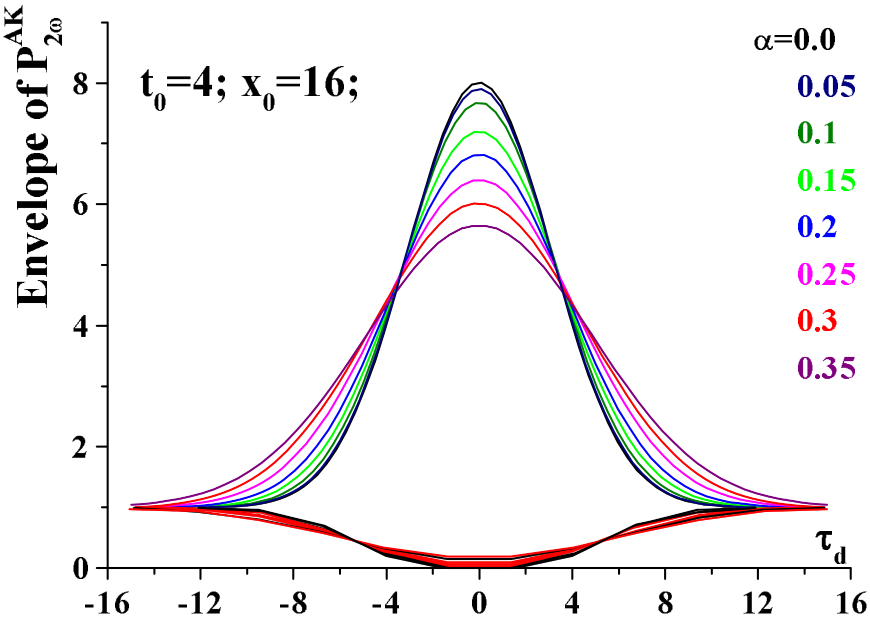

Fig. 6. Simulated envelopes of the interferometric atocorrelation signals (Eq. 13) for different values of the pulse front tilt α.

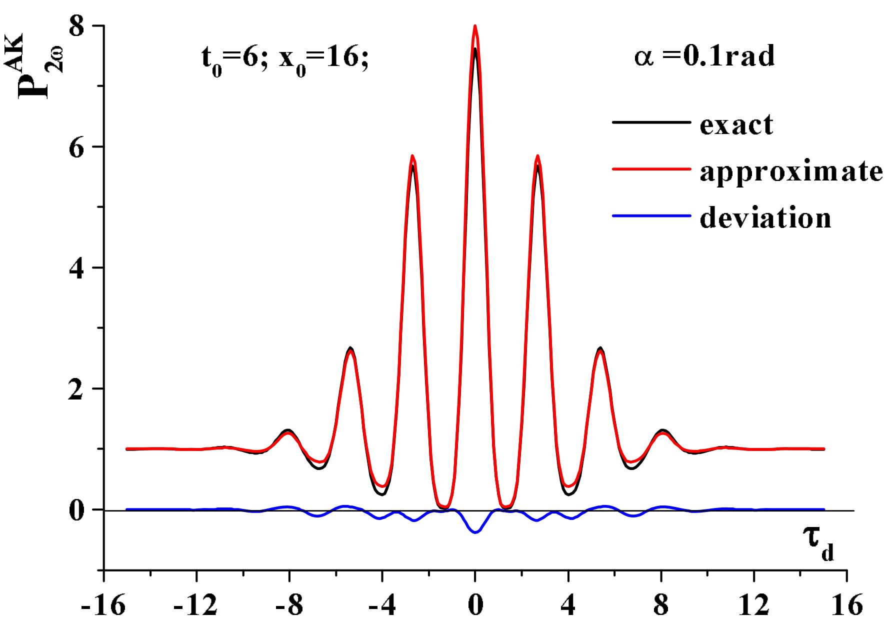

Fig. 7. Simulated interferometric atocorrelation signals by using the exact (Eq. 13) and the approximate analytical result (Eq. 15) and difference of the calculated signals (bottom curve) for pulse front tilt α=0.1rad.

Table 1. Relative pulse broadening Δt/Δt(α=0) for different pulse duration to beam width ratios vs. pulse front tilt angle α.

	Relative pulse broadening Δt/Δt(α=0)		
α [rad]	**t_0=2; x_0=16**	**t_0=4; x_0=16**	**t_0=6; x_0=16**
0	1	1	1
0.1	1.24	1.06	1.02
0.2	1.80	1.21	1.10
0.3	2.44	1.47	1.21

In the case of a relatively small pulse front tilt ($tan(\alpha) \approx sin(\alpha) \approx \alpha$) the derived general expression (13) simplifies to

$$P_{2\omega}^{AK} = 1 + 4\exp\left\{-\frac{4{\tau_d}^2}{3t_0^2}\right\} cos[\omega\tau_d] + \exp\left\{-\frac{{\tau_d}^2}{t_0^2 + x_0^2\alpha^2}\right\}\left(2 + cos[2\omega\tau_d]\right) . \tag{15}$$

The validity of this approximation has to be checked carefully. If the tolerable deviation of the approximate result from the exact one is within 5%, this approximate formula holds for α<100mrad (see Fig. 7). Since nearly single-cycle laser pulses require a lot of experimental effort and most of the misalignments of the optical system are probably compensated to reach this regime, Eq. 15 may appear a reasonable and relatively simple first-order approximation in analyzing autocorrelation signals in the presence of small pulse front tilts.

4. CONCLUSION

The presented results of the ray-pulse matrix analysis show that equally misaligned 4*f* and 2*f*-2*f* systems consisting of gratings and lenses of the same groove spacing/focal length introduce the same spatial chirp, group delay dispersion and time-vs.-angle coupling. Their signs depend solely on the sign of Δ. Even misaligned, the 4*f* system does not introduce pulse front tilt. Misaligned 2*f*-2*f* system introduces both pulse front tilt and angular chirp. Precisely aligned (Δ=0) 4*f* and 2*f*-2*f* systems remain dispersionless, chirpless and do not introduce time-vs.-angle coupling. We derived an exact and an approximate expression for the interferometric autocorrelation signal in the case of ultrashort laser pulses with arbitrary large pulse front tilts.

ACKNOWLEDGEMENTS

This work was supported by the National Science Fund (Bulgaria) under contract IRNI-17/2007.

REFERENCES

[1] Weiner, A. M., Heritage, J. P. and Kirschner, E. M., “High-resolution femtosecond pulse shaping,” J. Opt. Soc. Am. B 5, 1563-1572 (1988).

[2] Mariyenko, I. G., Strohaber, J. and Uiterwaal, G. J., “Creation of optical vortices in femtosecond pulses,” Optics Express 13, 7599–7608 (2005).

[3] Bezuhanov, K., Dreischuh, A., Paulus, G. G., Schätzel, M. G. and Walther, H., “Vortices in femtosecond laser fields,” Opt. Lett. 29, 1942–1944 (2004).

[4] Besuchanov, K., Dreischuh, A., Paulus, G. G., Schätzel, M. G., Walther, H., Neshev, D., Krolikowski, W. and Kivshar, Yu., "Spatial phase dislocations in femtosecond laser pulses," J. Opt. Soc. Am. B 23, 26-35 (2006).

[5] Kostenbauder, A. G., “Ray-Pulse matrices: A rational treatment for dispersive optical systems,” IEEE J. Quant. Electron. QE-26, 1148-1157 (1990).

[6] Duarte, F. J., “Multiple-prism dispersion and 4x4 ray transfer matrices,” Opt. Quant. Electron. 24, 49-53 (1992).

[7] Akturk, S., Gu, X., Gabolde, P. and Trebino, R., “The general theory of first-order spatio- temporal distortions of Gaussian pulses and beams,” Optics Express 13, 8642-8661(2005) and the references therein.

[8] Diels, J.-C. and Rudolph, W., [Ultrafast Laser Pulse Phenomena], Academic Press, London, 92-99 (1996).

[9] Grasbon, F., Dreischuh, A., Zacher, F., Paulus, G. G. and Walther, H., “Femtosecond interferometric autocorrelations in the presence of pulse front distortions,” Proc. SPIE, 3571, 164-168 (1999).

[10] Pretzler, G., Kasper, A. and Witte, K. J., “Angular chirp and tilted light pulses in CPA lasers,” Appl. Phys. B 70, 1–9 (2000).